

The Growth of Semiconductor Thin Films Studied by RHEED*

G. L. Price

Telecom Australia Research Laboratories,
770 Blackburn Rd, Clayton, 3168, Australia.

Abstract

Recent developments in the growth of semiconductor thin films are reviewed. The emphasis is on growth by molecular beam epitaxy (MBE). Results obtained by reflection high energy electron diffraction (RHEED) are employed to describe the different kinds of growth processes and the types of materials which can be constructed. MBE is routinely capable of heterostructure growth to atomic precision with a wide range of materials including III-V, IV, II-VI semiconductors, metals, ceramics such as high T_C materials and organics. As the growth proceeds in ultra high vacuum, MBE can take advantage of surface science techniques such as Auger, RHEED and SIMS. RHEED is the essential *in-situ* probe since the final crystal quality is strongly dependent on the surface reconstruction during growth. RHEED can also be used to calibrate the growth rate, monitor growth kinetics, and distinguish between various growth modes. A major new area is lattice mismatched growth where attempts are being made to construct heterostructures between materials of different lattice constants such as GaAs on Si. Also described are the new techniques of migration enhanced epitaxy and tilted superlattice growth. Finally some comments are given on the means of preparing large area, thin samples for analysis by other techniques from MBE grown films using capping, etching and liftoff.

1. Introduction

The development of the modern materials growth techniques of molecular beam epitaxy (MBE), metalorganic chemical vapour deposition (MOCVD) and their variants, has made routine the construction of materials, interfaces and surfaces to an atomic precision (Parker 1985; Herman and Sitter 1989). The purpose of this paper is to provide an overview of the growth processes and the kinds of materials which can be constructed. This will be done primarily by an account of reflection high energy electron diffraction (RHEED) research of the growth processes. This is not because it is the most powerful technique: for any given growth, a barrage of characterisation methods are conventionally applied. Some of these are transmission and scanning electron microscopy; optical microscopy; electronic characterisation by the Hall effect and deep level transient spectroscopy; optical characterisation by photoluminescence and optical modulation spectroscopies; stoichiometry, thickness and lattice matching by double crystal X-ray diffraction; and optical

* Paper presented at the Workshop on Interfaces in Molecular, Electron and Surface Physics, held at Fremantle, Australia, 4-7 February 1990.

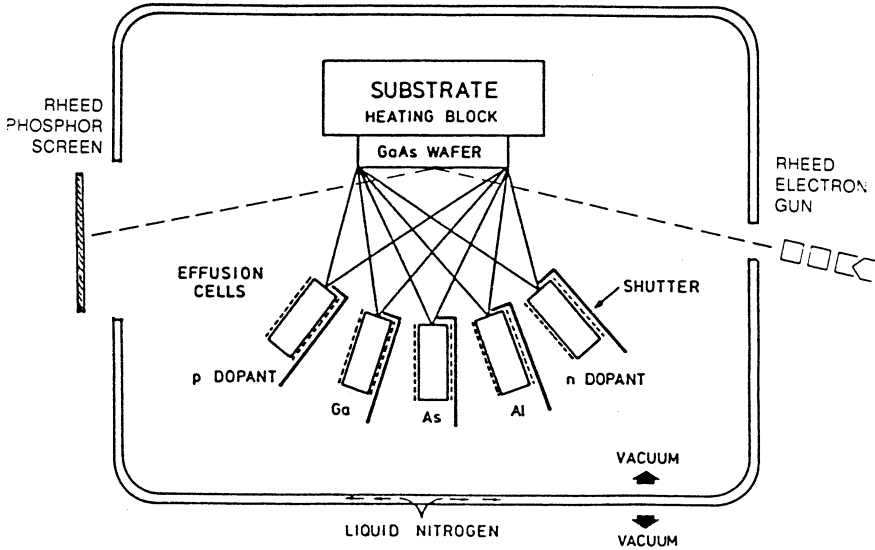


Fig. 1. Schematic diagram of an MBE system showing the RHEED geometry.

absorption and band edge measurements with Fourier infrared spectroscopy. RHEED of MBE growth is the only commonly used *in-situ* analysis technique. (Another is ellipsometry which is not yet widespread.) RHEED gives essential information as to the type of growth—layer by layer or island, the growth rate, the surface reconstruction and detailed knowledge of growth kinetics. RHEED is thus a useful vehicle for an overview and is an interesting technique in its own right. The treatment here will by no means be exhaustive; there is space only to sketch out some of the more active areas.

A schematic of an MBE machine is shown in Fig. 1. Elements of the required alloy are evaporated from the ovens onto a single crystal substrate. After some catalytic processes and surface diffusion, the elements combine in the correct stoichiometry and an epitaxial single crystal grows on the substrate—usually layer by layer. The rate of growth is about one atomic layer per second ($1 \mu\text{m}$ per hour). Mechanical shutters on the ovens provide an accuracy of 0.1 atomic layers. The RHEED beam (between 5 and 50 keV but conventionally 10 keV) strikes the crystal at a glancing angle of $<1^\circ$. Typical diffraction patterns observed on the phosphor screen are shown in Fig. 2. The ovens of Fig. 1 are shown for the growth of III-V compounds. Although much of the work to be described here deals with III-Vs, this is only because this has been the main application. MBE and RHEED are used with a wide range of materials including other semiconductors such as the group IVs and the II-VIs, all metal systems, high temperature superconductors and even organics.

The chief motivation for understanding the growth process has been to find ways of making better electronic and optoelectronic devices. In Fig. 3 are shown two device structures which can be made by the new materials growth techniques. Both have strict requirements on thickness and uniformity. The two dimensional electron gas layer may only be a few atomic layers thick.

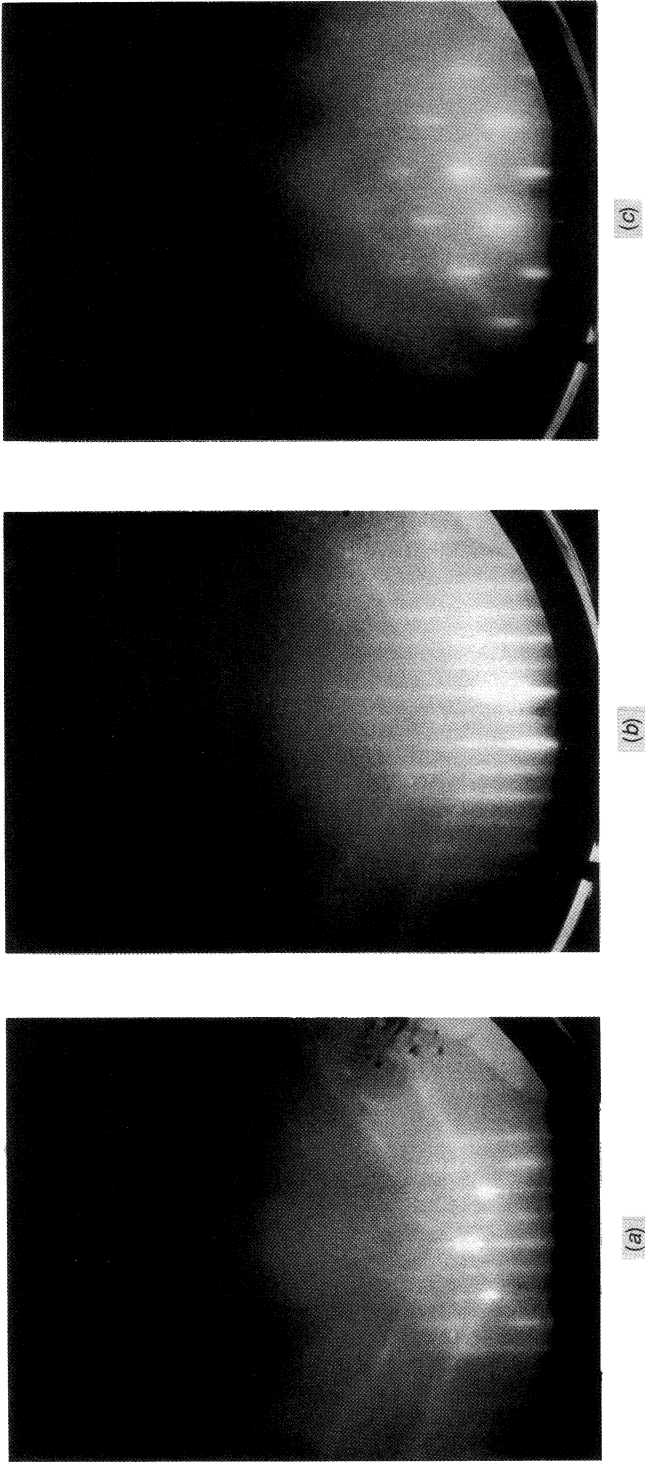


Fig. 2. RHEED diffraction patterns for (a) Annealed GaAs crystal: the diagonal streaks are Kikuchi lines. (b) During growth of GaAs: the rougher surface causes fine detail to be lost. (c) Three dimensional growth of InGaAs on GaAs.

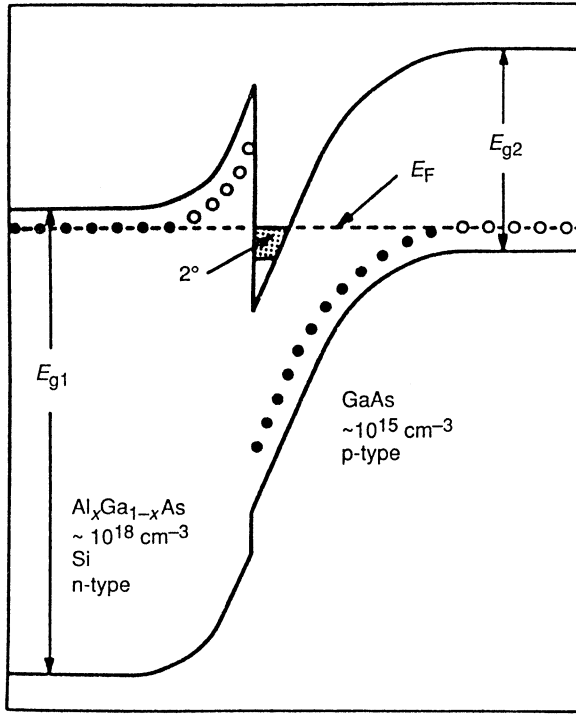


Fig. 3a. Band structure of a modulation doped GaAs/AlGaAs heterostructure; E_f and E_g are the Fermi and bandgap energies respectively. Electrons from the doped AlGaAs fill the part of the GaAs conduction band below E_f , forming a two-dimensional electron gas (after Stormer 1983).

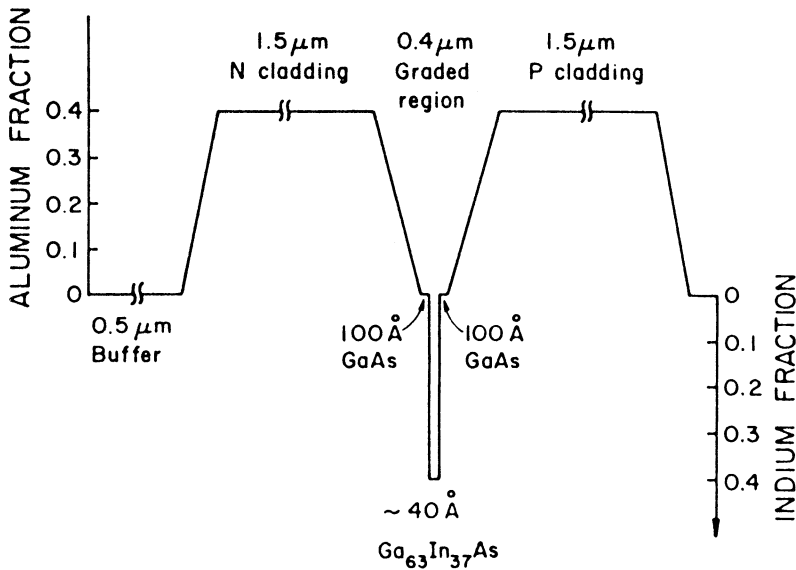


Fig. 3b. Conduction band of a strained layer InGaAs laser. The InGaAs active layer is only about six lattice constants thick (after Feketa *et al.* 1986).

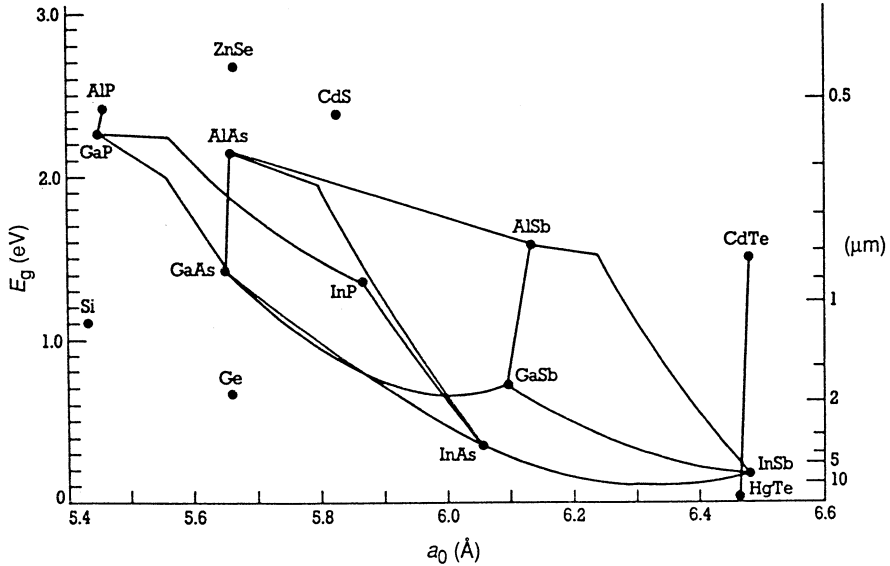


Fig. 4. Phase diagram of the III-Vs. Marked points are binaries, lines are ternaries and areas are quaternaries.

Such a heterostructure is the heart of modern devices like the high electron mobility transistor. Device uniformity demands the thickness be kept within 1% over an 8 cm wafer. That this can be attained and provide devices for consumer electronics is a measure of the technology's success. A strained layer laser structure is shown in Fig. 3*b*. This device is a successful example of a very active area of research in the last few years on the growth of lattice mismatched materials. Previously only lattice matched materials (to one part in 10^5) made useful devices. Mismatch stress results in extended defects which destroy the device properties of the materials. In this laser the InGaAs active layer has a larger lattice constant than GaAs and is compressively strained to the GaAs lattice. It is about six lattice constants thick and forms a quantum well which, when injected with carriers, emits light at $\sim 1 \mu\text{m}$ wavelength. Light of this wavelength can pass through GaAs which is useful for optical switching applications; it can also pump erbium doped fibre amplifiers (Wu *et al.* 1990). Another notable material is the 4% lattice mismatched system GaAs/Si which is an attempt to integrate III-V optoelectronics with consumer electronics. The phase diagram of Fig. 4 demonstrates this restriction of lattice matching. Only three materials have been developed sufficiently to use as large scale integrated substrates: Si, GaAs and InP. Thus the only lattice matched compounds which can be grown must lie on vertical lines passing through these three points. It is only a freak of the periodic table which gives Al approximately the same atomic radius as Ga and thus the constant lattice match of $\text{Al}_x\text{Ga}_{1-x}\text{As}$ to GaAs for all x . The ease of fabricating this heterostructure is a primary reason for the modern optoelectronics industry. An example of how the restrictions of this phase diagram can be bypassed by the growth of strained and lattice mismatched materials will be given later in this paper together with other new methods of thin film growth. First a brief summary of the useful attributes of RHEED will be given.

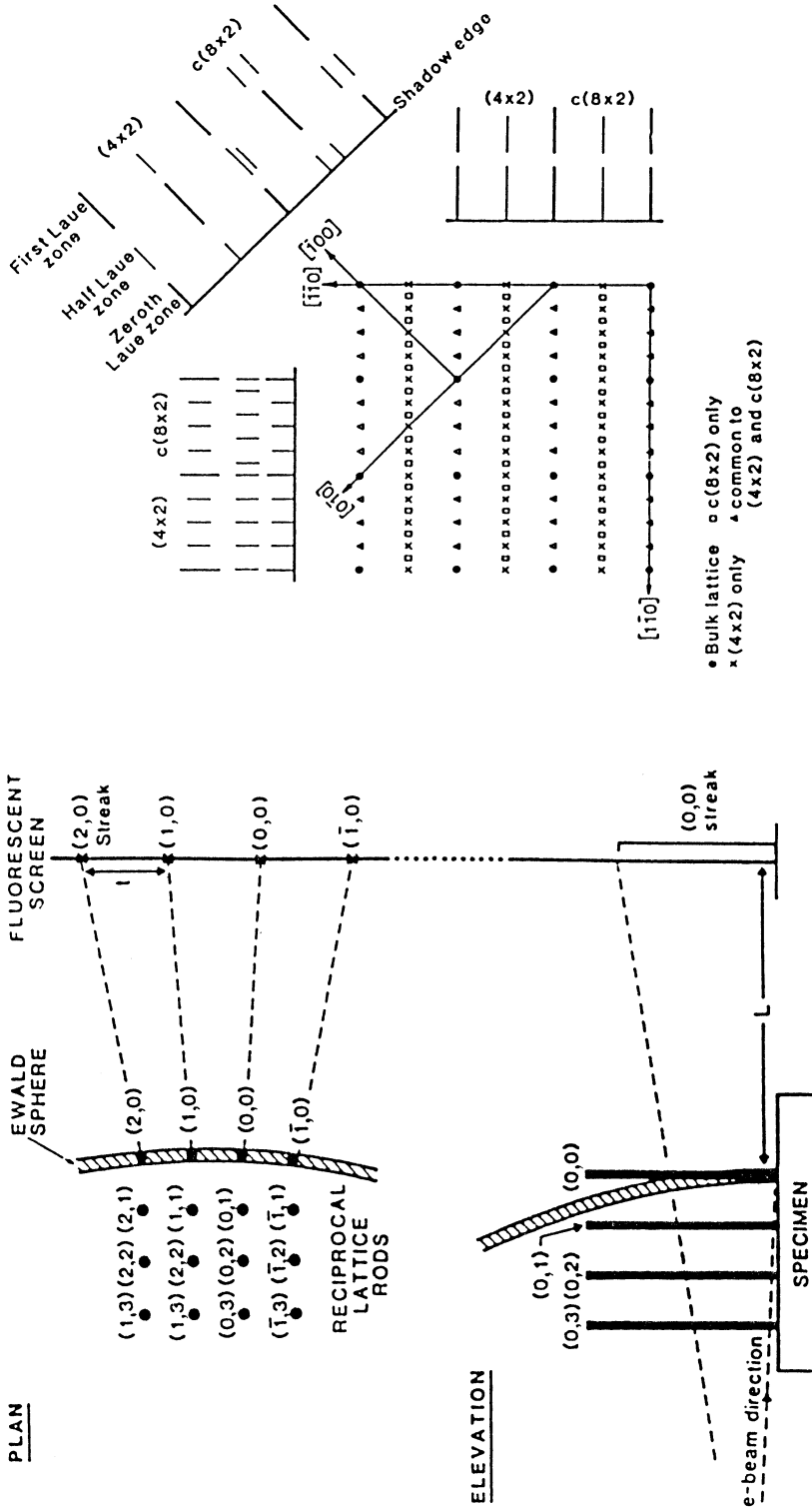


Fig. 5a. Sectioning of the two dimensional reciprocal lattice rods give the observed RHEED streaks (after Parker 1985).

Fig. 5b. Comparison of the LEED and RHEED patterns for the GaAs $c(8 \times 2)$ reconstruction (after Neave and Joyce 1978).

2. RHEED

The relation between the surface reciprocal lattice and the diffraction pattern is shown in Fig. 5a. The RHEED Ewald sphere takes a section through the surface rods and streaks are observed on the phosphor screen rather than the spots of the LEED case. To obtain the full reciprocal lattice map (given directly by LEED), the crystal substrate must be rotated about its normal; the Ewald sphere then sections each plane in turn. The LEED pattern shown in Fig. 5b is a complex gallium rich reconstruction referred to as the centred 8×2 . The three main azimuths which should be observed in RHEED are also drawn. The fine detail of the 8th order is rarely seen with RHEED and the pattern is referred to as a 4×2 . Practically this is of little consequence as the growth conditions are established to avoid this reconstruction by decreasing the metal/arsenic ratio and obtaining the arsenic rich 2×4 (LEED $c(2 \times 8)$). The fine detail is not required for when this transition from metal to arsenic rich reconstruction occurs, the four streaks of the $[110]$ change to two (Fig. 2a). If the surface roughens, then transmission rather than reflection patterns are obtained as shown in Fig. 2c. The beam, skimming over the surface, penetrates peaks and ridges. The streaks are replaced with points since the surface reciprocal lattice rods are now replaced by the reciprocal lattice itself.

The depth sensitivity of RHEED is of order of an atomic layer. It can be estimated from $\lambda \sin(\gamma)$ where $\gamma \sim 1^\circ$ is the glancing angle and where λ is the electron mean free path ~ 20 nm at 10 keV. The electron wavelength is ~ 0.01 nm which is an order of magnitude smaller than an atomic layer. Thus the diffraction is sensitive to the surface and the electrons are easily scattered by surface steps and terraces. The diffraction, like LEED, is dominated by multiple scattering and simple kinematic arguments cannot be applied to the streak intensities. The lateral sensitivity of RHEED is of order 100 nm. Variations in RHEED streaks have been attributed to monoatomic steps 200 nm apart on a GaAs crystal (Pukite *et al.* 1984). This does not necessarily give good sensitivity to disorder. Disorder gives a diffuse background spread over a large solid angle. Large increases in this background have little effect on the sharp, high intensity diffraction features. Thus the diffraction process selects out the ordered parts of the surface. For this reason, and because of the beam spread across the crystal, RHEED can often give a good diffraction pattern off a patchy or dirty surface.

Growths which give RHEED streaks, not spots, have a two dimensional nucleation and growth behaviour. This means that the adatoms remain in the same plane. At the initial stages of growth on an atomically flat surface, the adatoms migrate over distances measured by a migration length $l = l_0 \exp(-E_1/kT)$ where E_1 is the migration energy. The adatoms are scavenged by a number of processes such as nucleation where an island is formed with other adatoms; step propagation—binding to a step which can be the side of an island or a substrate terrace; and desorption. Three dimensional growth involves adatoms jumping up on top of islands and forming three dimensional crystals which give rise to RHEED spots.

RHEED can calibrate these two-dimensional growths and give detailed information on surface migration kinetics. As growth proceeds, the specular beam oscillates in intensity, the period of the oscillations being equal to the time taken to grow a single monolayer of material. Typical oscillations are

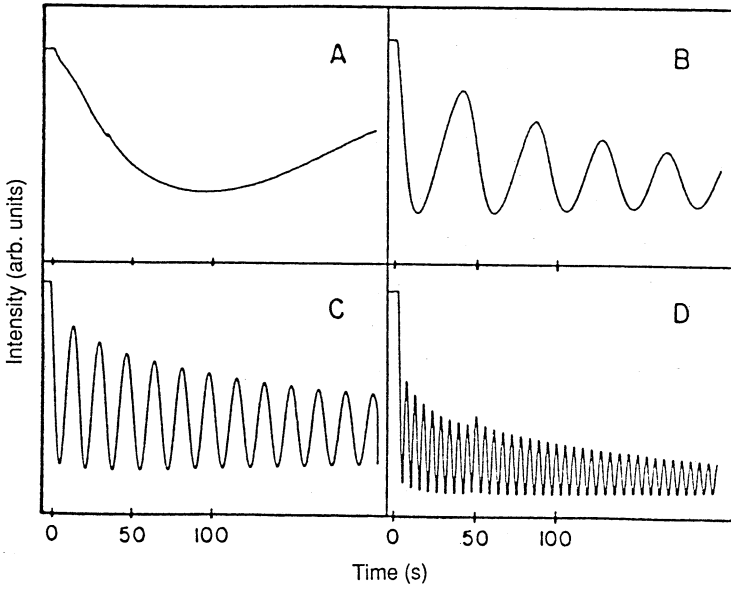


Fig. 6. Observed RHEED oscillations on a GaAs crystal for increasing flux rates. In A the flux is so slow that the substrate steps can scavenge the adatoms before nucleation. The vicinal angle is 1.0 mrad (after Van Hove and Cohen 1987).

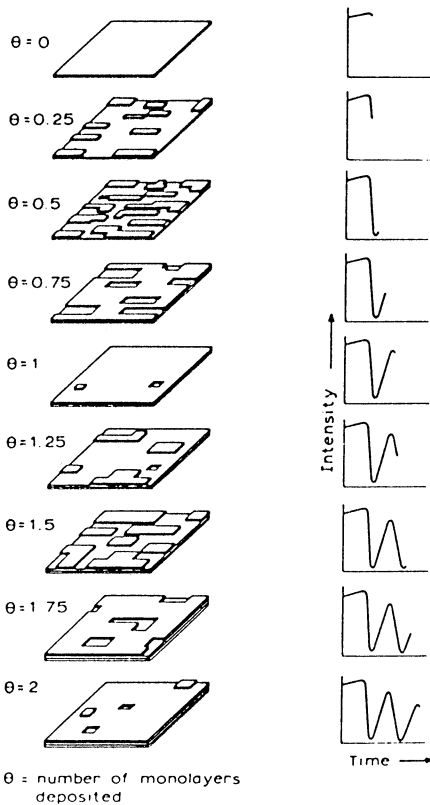


Fig. 7. A first order growth model of the intensity oscillations (after Joyce *et al.* 1986).

shown in Fig. 6 and a schematic explanation is given in Fig. 7. The first few layers are essentially complete before another begins. Since the layer thickness is much larger than the de Broglie wavelength of the electrons (for GaAs $0.283 \text{ nm} \gg 0.01 \text{ nm}$), the electrons are easily scattered out of the specular beam by the step edges. The step edge concentration is a minimum for a completed layer and a maximum for half a monolayer coverage—hence the oscillations. This simple explanation must be modified to explain the damping of the oscillations as the growth continues. If adatoms fall in a “ravine” between two steps of width less than the migration length, they will be gettered by the step edges and nucleation and creation of more step edges will not be possible. As the coverage increases this becomes more likely but so does nucleation of a second layer on top of the first. The result is an increase in the concentration of step edges with growth, tending to a limiting equilibrium value. In RHEED this is seen by the damping of the oscillations and their disappearance corresponds to the steps getting all arriving adatoms. A good illustration of this process is shown in Fig. 8. Al has a smaller migration length than Ga. GaAs is grown until there are no oscillations. When the aluminium is added oscillations are seen again as the smaller migration length enables nucleation. When the Al is removed, nothing happens as the growth continues to be by step propagation. An estimate of the migration length can be found by growing at a fixed flux for differing temperatures on a vicinal surface. On such a surface, cut at a slight angle to a (100) plane, there are terraces of known length. The result is shown in Fig. 9. The migration length increases with temperature, and at a certain temperature T_c , growth is only by step propagation. From this, values of l_0 and E_1 can be derived. One estimate for Ga atoms on a GaAs (100) surface is $l_0 = 0.4 \text{ nm}$ and $E_1 = 0.3 \text{ eV}$ (Shitara and Nishinaga 1989) giving less than $0.05 \mu\text{m}$ migration lengths for normal growth temperatures up to 640°C . However a recent experiment has given conflicting results (Nilsson *et al.* 1989). A set of four AlGaAs/GaAs/AlGaAs quantum wells were grown successively on a substrate which had been etched to expose a (311)A facet about $1 \mu\text{m}$ deep. The quantum well thicknesses were measured by spectral resolved cathodoluminescence in an SEM and were found to increase exponentially along the (100) surface up to the intersection of the (100) and the (311). Incident atoms had diffused preferentially from the (311) onto the (100) and so the (311) acted as a source of Ga for the (100). A migration length of 1 to $2 \mu\text{m}$ was deduced from this exponential rise.

3. Migration Enhanced Epitaxy

In normal MBE growth, the equilibrium number of step edges gives heterostructure interfaces which are rough on an atomic scale. There is also a need for good quality growths at lower temperatures both to sharpen impurity profiles and bypass regions of island growth. Higher growth temperatures have the disadvantage of poorer impurity profiles and more difficult growth conditions. Methods used have included growth on vicinal surfaces to ensure step-flow growth; growth interruption to allow surfaces to anneal; and various photon and ionised particle irradiation techniques which provide energy to enhance surface migration. A simple and effective technique was recently invented (Horikoshi *et al.* 1988) which greatly enhances the surface mobility at

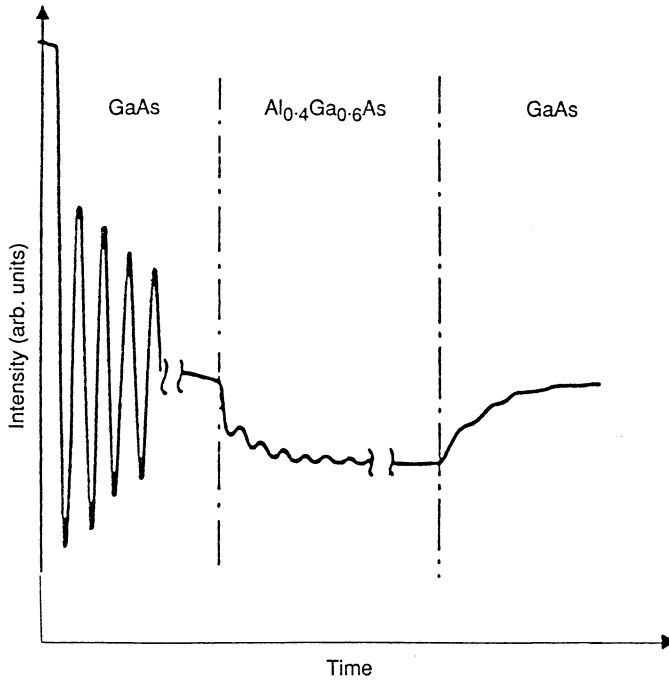


Fig. 8. Intensity oscillations across GaAs/AlGaAs/GaAs interfaces. The short migration length of the Al restarts the oscillations (after Joyce *et al.* 1988).

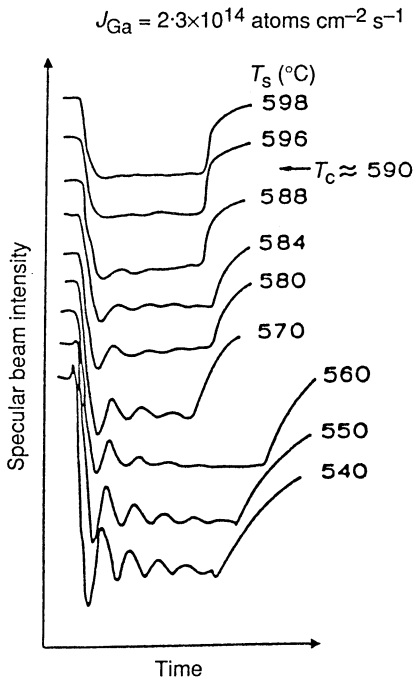


Fig. 9. Growth of GaAs on a vicinal surface as a function of temperature. At T_c the migration length is of order of the step separation (after Dobson *et al.* 1987).

all temperatures for III-V compounds. Known as migration enhanced epitaxy (MEE), it uses the high mobility of a Ga atom compared with a GaAs molecule when migrating on either a Ga or an As surface. Layers of Ga and As are layed down alternately instead of being supplied simultaneously to the growth surface. As has a negligible sticking coefficient unless there is available Ga. Ga has metallic bonding to a Ga plane and migration is easy. On an As plane, Ga has an unsatisfied bond perpendicular to the surface whose strong acceptor nature is thought to destabilise the two other bonds and enhance migration. In contrast, the diffusion of a GaAs molecule requires its dissociation which takes a few eV. Using MEE, it is found that growths below 300°C are of equivalent quality to those at 600°C.

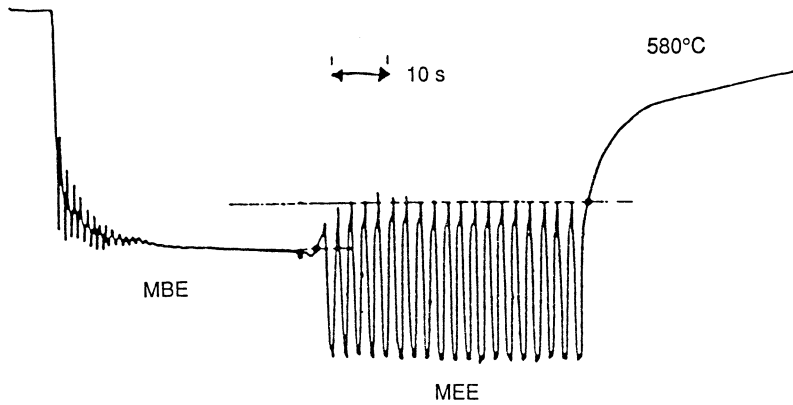


Fig. 10. RHEED oscillations by MBE followed by MEE. The same 2×4 reconstruction remained through the growth (after Horikoshi *et al.* 1988).

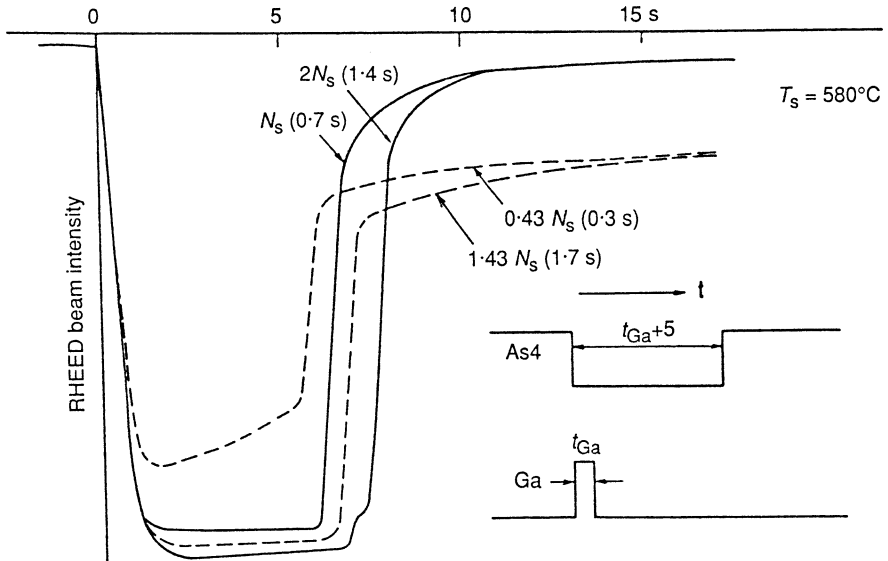


Fig. 11. RHEED specular beam intensity for alternate deposition of Ga and As₄ as shown in the inset (after Horikoshi *et al.* 1989).

surface is established. Without them, the sublayer would be incomplete and the surface rough.

If MEE and step-flow growth are combined on a vicinal surface, heterostructures with interfaces normal or angled to the substrate can be created. Fig. 12 demonstrates the method. A GaAs surface cut at 2° from [001] towards the [110] gives a terrace with 80 Å step widths and with the As dangling bonds parallel to the step edges. The AlAs occupies the first part of the step and the GaAs the second. MEE was used to gain the highest mobility. The tilt angle β can be adjusted by altering the ratio of Ga to Al. More recent experiments have shown that depositing Ga and Al simultaneously produces a spontaneous composition modulation with the Al rich regions preferentially forming at the bottom of steps (Tsuchiya *et al.* 1989).

Quantum wires can be made from these superlattices by confining the GaAs top and bottom with AlAs. Long wires of dimension 10 nm are then formed which constrain the carriers to one-dimensional physics. Applications are to high mobility electron devices (Tsubaki *et al.* 1988), electron interference devices which rely on the superlattice period coinciding with the carrier wavelengths and optoelectronics which takes advantage of the small dimensions to strongly confine electron and holes.

4. Lattice Mismatched Growth

The control over materials growth previously described has been applied to lattice mismatched growth in an endeavour to create quite new materials and to access the full range of a given phase diagram like Fig. 4. It is well known that when a slightly incommensurate material is grown on a substrate, it will strain to conform to the substrate lattice constant. Such pseudomorphic growth continues until a critical thickness is reached where the strain energy in the growing film is sufficient to force misfit dislocations to accommodate the strain. There has been continuing controversy over the critical thickness in various systems. Much of the discussion is concerned with relatively low strained films (<0.020) where plasticity effects and probe resolution complicate the interpretation of results. In this section, an account will be given of the application of RHEED to highly strained films (>0.025). This is a region of considerable technological interest (e.g. InGaAs/GaAs long wavelength lasers, GaAs/Si) and since the critical thicknesses are only a few atomic layers, the films are not easily characterised by normal electrical or optical methods. For these highly strained films, RHEED can give information on both strained epilayers and quantum wells.

The surface lattice constant and hence the surface strain is inversely proportional to the separation of the RHEED streaks. In Fig. 13 this strain is plotted against film thickness for different multiquantum well (MQW) structures. Both MQWs have five periods, one with a 2.4 nm $\text{In}_{0.4}\text{Ga}_{0.6}\text{As}$ well and the other with a 6.0 nm well. The substrate and the well barriers (23.9 nm thick) are GaAs. The surface strain is $(a_0 - a_s)/a_0$ where a_0 and a_s are the lattice constants of the surface of the overlayer and the substrate respectively. Curves are given for the first, second and fifth period of each MQW structure. The curves for the 2.4 nm MQW have four regions. Initially the InGaAs grows pseudomorphically on the GaAs and the RHEED streak spacing of the InGaAs

is that of the GaAs substrate. After the critical thickness (h_c) is reached (five atomic layers), there is a transition over an atomic layer as the InGaAs relaxes. The streaked RHEED pattern changes to spots and the growth is three dimensional. If the InGaAs growth is left to proceed, the surface strain stays constant, the islands coalesce and a streaked pattern gradually begins to form again as the InGaAs smooths. In Fig. 13, after 2.4 nm, the indium is switched off and a GaAs barrier is grown. The surface strain moves quickly back to that of GaAs. The 6.0 nm MQW behaviour is similar.

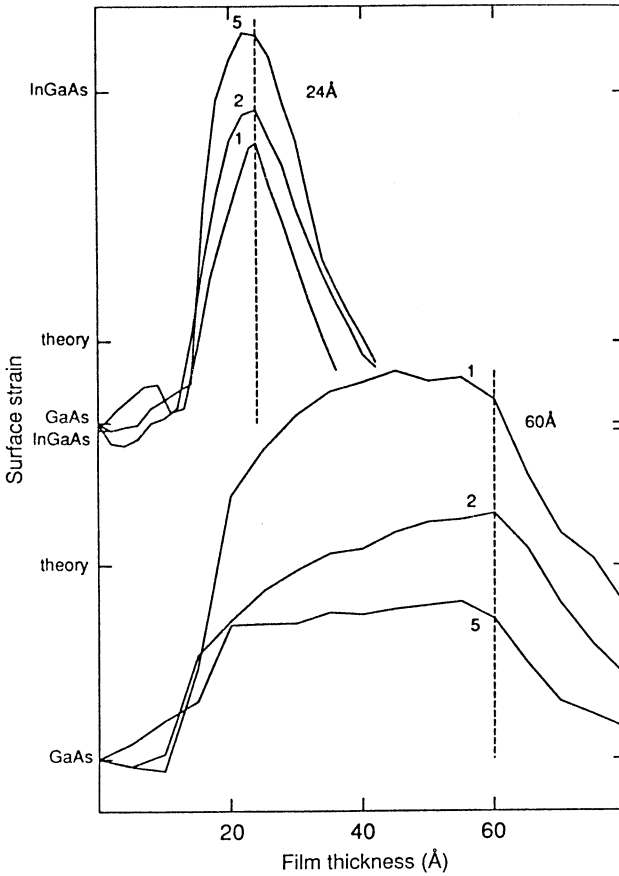


Fig. 13. Surface strain found by RHEED versus film thickness for the first, second and fifth periods of 2.4 nm and 6.0 nm MQW structures. The abscissa zero is the beginning of the InGaAs layer. The dotted line marks the commencement of the GaAs barrier. The surface strain for equilibrium $\text{In}_{0.4}\text{Ga}_{0.6}\text{As}$ and the surface strain change predicted by theory for the bulk film are marked on the ordinate for both structures (after Price and Usher 1989).

The first important result found with RHEED is the critical thickness. The onset of the transition can be measured easily to an atomic layer. If this is identified as the critical thickness, then by varying the indium concentration

a comparison with theory such as Fig. 14 can be made. The theories of pseudomorphic growth assume that at the critical thickness the elastic strain is sufficient to enable dislocations to accommodate some of the lattice misfit and lower the stress. The theories divide into homogeneous and heterogeneous dislocation nucleation and are further subdivided by different dislocation mechanisms. The greatest difference is between the homogeneous and the heterogeneous. The heterogeneous theory assumes no nucleation energy is required before dislocations can exist in the film and is derived by equating forces on dislocations. The homogeneous theory equates energy of dislocation formation with the strain energy of the film. The experimental points clearly fit the heterogeneous theory and are closest to the theory which assumes misfit accommodation by 60° dislocations. An interesting aspect of these results is that the surface energy of the film must be included for such thin films.

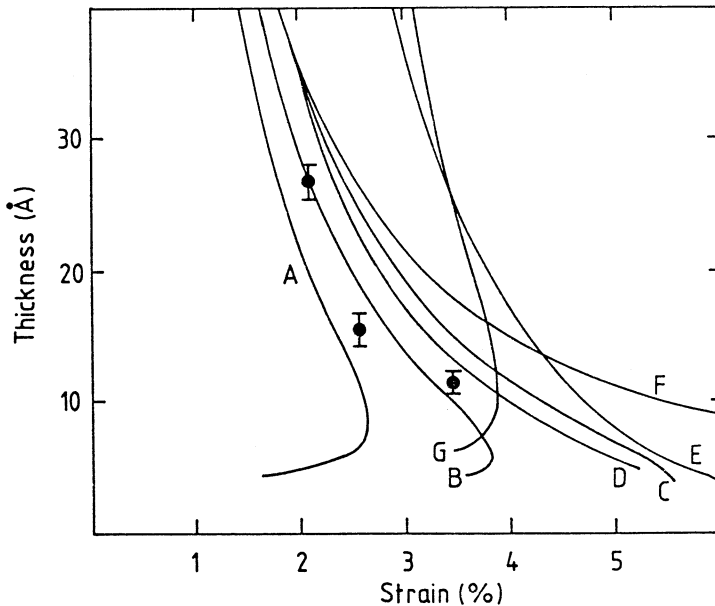


Fig. 14. Critical thicknesses determined by RHEED for InGaAs on GaAs for three misfits and compared with theory: A, B and C are for 60° dislocations with surface energy 1.0 , 0.5 , and 0 J m^{-2} , respectively; D is for Frank partials; E is the homogeneous nucleation of Shockley half loops and F is the film thickness required to accommodate them; G is for the homogeneous nucleation of screw dislocations (after Price 1988a).

Of equal importance to the heterostructure is the critical thickness of quantum wells (h_q). Simple theory predicts that the quantum well will withstand twice the stress of the single heterostructure because of the support of the two well walls. It follows that $h_q > h_c$. There is thus a region as the quantum well is grown where h_c is exceeded, introducing dislocations with island growth. For a defect free quantum well, the growth of the second wall must reversibly remove these defects. The results of Fig. 13 were obtained to investigate this region and to determine if RHEED had the sensitivity to measure h_q . For

the 2.4 nm MQW, the transition increases with period. Previous experiments have demonstrated that the strength of the transition is dependent on crystal quality. Hence the crystal improves as more strained quantum wells are grown. This improvement is well known and strained layer MQWs are often employed to quickly prepare substrates before growth. The 6.0 nm MQW on the other hand degrades. This is attributed to h_q being exceeded. It thus falls between these extremes and by varying the well thickness h_q can be estimated. Double crystal x-ray diffraction of the grown MQW confirmed these results. The fact that for $h_c < h < h_q$, excellent quantum wells are obtained, shows that the defects introduced after h_c are removed by the GaAs cap.

There are many unknown areas in the growth of these highly strained layers. The theory assumes dislocations accommodate the misfit but the uncertainty in the core energy, especially in such thin films, is very large so agreement with theory does not establish the type of defect. Recently quite new types of defects have been found. One is for Ge/Si(100) which has a strain of 4% (LeGoues *et al.* 1989). The Ge was forced to grow layer by layer by terminating the surface with As during growth. Normally it forms islands after three layers. The As saturated the surface dangling bonds and the Ge grew underneath the segregating As surface layer. The bond saturation prevented island formation to 15 monolayers. The new defects are broad V shaped regions of distorted crystal 4.5 atomic planes thick with estimated energy values similar to dislocations. Other active areas of investigation include the mechanism of dislocation nucleation and multiplication, particularly as far as determining if dislocations nucleate at the surface of the growing film; the detailed reasons for the transition to island growth and the large question of the temperature dependence and plasticity effects in these strained layers. There is not space to deal with these questions here which are largely unresolved, but some insight into the balance between homogeneous and heterogeneous nucleation has been given by the potentially technologically useful technique of patterned growth.

A typical substrate may have $\sim 5 \times 10^4$ dislocations per cm^2 . If this substrate is etched to form a pattern of square mesas, say 80 μm on side and 25 μm apart, then there will only be on average one dislocation in each mesa. It is the interaction between dislocations in the case of low strained films which causes the heterogeneous accommodation of misfit as described above for InGaAs on GaAs. The troughs between the islands prevent this interaction. This has been demonstrated experimentally for GeSi/Si and InGaAs/GaAs by cathodoluminescence (Fitzgerald *et al.* 1988). They have observed individual dislocations in mesas and by decreasing the mesa size, decreased the dislocation density. For low strain films where only heterogeneous accommodation is present, large increases in the critical thickness should occur as the film must grow until its elastic energy is sufficient to homogeneously nucleate dislocations. This increase is theoretically predicted to be up to an order of magnitude (extrapolation of curves B and E to greater thickness in Fig. 14). As the strain increases over 2%, misfit accommodation processes which are not area dependent are expected to reduce this advantage. Again RHEED can be used for these highly strained films and a doubling of the critical thicknesses for 70 μm square mesas and $\text{In}_{0.3}\text{Ga}_{0.7}\text{As}$ epilayers have been

observed. As the indium concentration increases, the effect decreases; there is no difference between a simultaneously grown patterned and unpatterned substrate for $\text{In}_{0.4}\text{Ga}_{0.6}\text{As}/\text{GaAs}$ (Price 1988*b*).

5. Materials Preparation

To conclude, some comments will be given on preparing the types of materials that have been described above for examination by other techniques which require either very thin samples such as (e,2e) and transmission electron microscopy or which need a clean surface like photoelectron spectroscopy or scanning tunnelling microscopy.

A well tested method for preserving the surface has been the capping with As when dealing with the III-Vs (Kowalczyk *et al.* 1981; Price 1982). After growth, the specimen is cooled below 100°C for As_2 deposition or below 0°C for As_4 . It can then be stored in air for long periods before being placed again in a uhv chamber. Warming the sample desorbs the As cap at about 350°C, leaving the original surface with the $c(2\times 8)$ reconstruction. Auger, ESCA and UPS have confirmed the cleanliness of this technique.

Conventional methods of preparing thin samples include wet etching, ion beam thinning and microtome. Etchants are available which have a selectivity between materials of 10^7 , e.g. they can etch quickly through AlGaAs but effectively stop on GaAs. It is thus possible to obtain a thin film in a well supported matrix. A new technique of thin film liftoff has recently been used for device work and sample preparation (Yablonovitch *et al.* 1987; Joyce and Dell 1990; Breen *et al.* 1989). An AlAs "release" layer, 2 to 50 nm thick is first grown on a GaAs substrate. The device or layer which is required is then grown epitaxially on the AlAs. The sample is removed and coated with "Apiezon W" wax and etched in HF at a few degrees below zero. This selectively etches the AlAs and the layer floats to the surface. The wax can be removed with trichlorethylene. The thinnest films reported so far are 50 nm but there does not appear to be any barrier other than a delicate experimental technique to preparing films of 10 nm thickness required for (e,2e). The wax removal is so effective that the films can be returned to the MBE as substrates for further growth. This in turn opens up a new materials area where strained layers are released from their substrates and allowed to relax. They are then bonded by Van der Waals forces onto the same or different substrate and used as a new substrate material with a different lattice constant from the Si, GaAs or InP standards. If successful, this technique will dramatically lessen the restrictions of lattice matching (Fig. 4).

Acknowledgment

This paper is published with the permission of the Executive General Manager, Research.

References

- Breen, K. R., Uppal, P. N., and Ahearn, J. S. (1989). *J. Vac. Sci. Technol. B* **7**, 758.
- Dobson, P. J., Joyce, B. A., Neave, J.H., and Zhang, J. (1987). *J. Cryst. Growth* **81**, 1.
- Feketa, D., Chan, K. T., Ballantyne, J. M., and Eastman, L. F. (1986). *Appl. Phys. Lett.* **49**, 1654.

- Fitzgerald, E. A., Watson, G. P., Proano, R. E., Ast, D. G., Kirchner, P. D., Petit, G. D., and Woodall, J. M. (1989). *J. Appl. Phys.* **65**, 2220.
- Gaines, J.M., Petroff, P.M., Kroemer, H., Simes, R. J., Geels, R. S., and English, J. H., (1988). *J. Vac. Sci. Technol. B* **6**, 1378.
- Herman, M. A., and Sitter, H. (1989). 'Molecular Beam Epitaxy' (Springer: Berlin).
- Horikoshi, Y., Kawashima, M., and Yamaguchi, H. (1988). *Jap. J. Appl. Phys.* **27**, 169.
- Horikoshi, Y., Yamaguchi, H., and Kawashima, M. (1989). *Jap. J. Appl. Phys.* **28**, 1307.
- Joyce, B. A., Dobson, P. J., Neave, J. H., Woodbridge, K., Zhang, J., Larsen, P. K., and Bolger, B. (1986). *Surf. Sci.* **168**, 423.
- Joyce, B. A., Zhang, J., Neave, J. H., and Dobson, P. J. (1988). *App. Phys. A* **45**, 255.
- Joyce, M. J., and Dell, J. M. (1990). *Phys. Rev. B*, accepted for publication.
- Kowalczyk, S.P., Miller, D. L., Waldrop, J. R., Newman, P. G., and Grant, R. W. (1981). *J. Vac. Sci. Tech.* **19**, 255.
- LeGoues, F. K., Copel, M., and Tromp, R. (1989). *Phys. Rev. Lett.* **63**, 1826.
- Neave, J. H., and Joyce, B. A. (1978). *J. Cryst. Growth* **44**, 387.
- Nilsson, S., Van Gieson, E., Arent, D. J., Meier, H. P., Walter, W., and Forster, T. (1989). *Appl. Phys. Lett.* **55**, 972.
- Parker, E. H. C. (ed) (1985). 'The Technology and Physics of Molecular Beam Epitaxy' (Plenum: New York).
- Pashley, M. D., Haberern, K. W., Friday, W., Woodall, J. M., and Kirchner, P. D. (1988). *Phys. Rev. Lett.* **60**, 2176.
- Price, G. L. (1982). 'Collected Papers of the Second International Symposium on Molecular Beam Epitaxy and Clean Surface Techniques', p. 259 (Japan Soc. Appl. Phys.: Tokyo).
- Price, G. L. (1988a). *Appl. Phys. Lett.* **53**, 1288.
- Price, G. L. (1988b). unpublished.
- Price, G. L., and Usher, B. F. (1989). *Appl. Phys. Lett.* **55**, 1984.
- Pukite, P. R., Van Hove, J. M., and Cohen, P. I. (1984). *J. Vac. Sci. Technol. B* **2**, 243.
- Shitara, T., and Nishinaga, T. (1989). *Jap. J. Appl. Phys.* **28**, 1212.
- Stormer, H. L. (1983). *Surf. Sci.* **132**, 519.
- Tsubaki, K., Fukui, T., Tokura, Y., Saito, H., and Susa, N. (1988). *Electr. Lett.* **24**, 1267.
- Tsuchiya, M., Petroff, P. M., and Coldren, L. A. (1989). *Appl. Phys. Lett.* **54**, 1690.
- Van Hove, J. M., and Cohen, P. I. (1987). *J. Cryst. Growth* **81**, 13.
- Wu, M. C., Olsson, N. A., Sivco, D., and Cho, A. Y. (1990). *Appl. Phys. Lett.* **56**, 221.
- Yablonovitch, E., Gmitter, T. J., Harbison, J. P., and Bhat, R. (1987). *Appl. Phys. Lett.* **51**, 2222.
- Yamada, K., Inoue, N., Osaka, J., and Wada, K. (1989). *Appl. Phys. Lett.* **55**, 622.